THE JOURNAL OF BIOLOGICAL CHEMISTRY VOL. 290, NO. 1, pp. 409–422, January 2, 2015

Up-regulation of Thrombospondin-2 in Akt1-null Mice Contributes to Compromised Tissue Repair Due to Abnormalities in Fibroblast Function*

Received for publication, October 12, 2014, and in revised form, November 11, 2014 Published, JBC Papers in Press, November 11, 2014, DOI 10.1074/jbc.M114.618421

Tara Bancroft[‡§], **Mohamed Bouaouina**[¶], **Sophia Roberts**[§], **Monica Lee**[§‖], **David A. Calderwood**[§¶‖], **Martin Schwartz**[§**], **Michael Simons**[§**], **William C. Sessa**[§‖], **and Themis R. Kyriakides**[‡§‡‡1]

From the Departments of [‡]*Pathology,* [¶]*Cell Biology,* [‖]*Pharmacology,* [**]*Cardiology, and* [‡‡]*Biomedical Engineering and the* [§]*Program of Vascular Biology and Therapeutics, Yale University School of Medicine, New Haven, Connecticut 06520*

Background: TSP2 and Akt1 exert opposite effects on tissue repair.
Results: Akt1 KO mice display defects in fibroblast morphology and adhesion due to diminished Rac activation, which is a result of increased TSP2 expression. Loss of TSP2 rescues these defects.
Conclusion: TSP2 contributes to compromised tissue repair in Akt1 KO mice.
Significance: These data support a novel, NO-independent TSP2 regulatory mechanism in fibroblasts.

Vascular remodeling is essential for tissue repair and is regulated by multiple factors, including thrombospondin-2 (TSP2) and hypoxia/VEGF-induced activation of Akt. In contrast to TSP2 knock-out (KO) mice, Akt1 KO mice have elevated TSP2 expression and delayed tissue repair. To investigate the contribution of increased TSP2 to Akt1 KO mice phenotypes, we generated Akt1/TSP2 double KO (DKO) mice. Full-thickness excisional wounds in DKO mice healed at an accelerated rate when compared with Akt1 KO mice. Isolated dermal Akt1 KO fibroblasts expressed increased TSP2 and displayed altered morphology and defects in migration and adhesion. These defects were rescued in DKO fibroblasts or after TSP2 knockdown. Conversely, the addition of exogenous TSP2 to WT cells induced cell morphology and migration rates that were similar to those of Akt1 KO cells. Akt1 KO fibroblasts displayed reduced adhesion to fibronectin with manganese stimulation when compared with WT and DKO cells, revealing an Akt1-dependent role for TSP2 in regulating integrin-mediated adhesions; however, this effect was not due to changes in β1 integrin surface expression or activation. Consistent with these results, Akt1 KO fibroblasts displayed reduced Rac1 activation that was dependent upon expression of TSP2 and could be rescued by a constitutively active Rac mutant. Our observations show that repression of TSP2 expression is a critical aspect of Akt1 function in tissue repair.

Angiogenesis is the formation of blood vessels from pre-existing vessels and is important in development and tissue repair. A delicate balance between intracellular and cell- and matrix-bound pro- and anti-angiogenic factors dictates the angiogenic response (1–8). Akt1/PKBα and TSP2 are well characterized as pro- and anti-angiogenic factors, respectively, whose expression is inversely related (9–12) and exert opposite effects on the outcome of tissue repair.

TSP2 is an anti-angiogenic matricellular protein that is part of a small family of five related glycoproteins called the thrombospondins (13). It is secreted upon injury and binds to the surrounding extracellular matrix (ECM)[2] to exert its cellular effects, primarily through interactions with cell surface integrins, low density lipoprotein receptor-related protein 1 (LRP1), CD36, and CD47 (13–17). Studies in knock-out mice have provided insight into the significance of these interactions. Specifically, TSP2 KO mice displayed increased blood flow recovery following hind limb ischemia associated with improved angiogenesis and arteriogenesis (18), accelerated wound healing (19–21), and altered foreign body response (22, 23). TSP2 contributes to the remodeling stage of wound repair by binding to and increasing cellular uptake of MMP2 and MMP9. Therefore, in its absence, increased MMP2/9 in the matrix allows for enhanced endothelial cell (EC) migration and chord formation, resulting in increased neovascularization and altered ECM organization (18, 21). Other possibilities for the mechanism of action of TSP2 include binding of CD36 to induce EC apoptosis and blockade of NO signaling in ECs through interaction with CD47 (24, 25).

TSP2 is not typically expressed at high levels in uninjured tissues, including blood vessels (9, 10, 18, 20), but can be induced after injury, with levels peaking at 10 days of wound healing. TSP2 is undetectable in platelets and endothelial cells, making fibroblasts the primary TSP2 producers *in vivo* in WT mice (20). TSP2 is known to influence several cell functions, including adhesion, migration, and contraction of matrix (21, 26). In tissue remodeling and neovascularization, the ability of

* This work was supported, in whole or in part, by National Institutes of Health Grant HL 107205 (to T. R. K., W. C. S., M. S., and M. A. S.). This work was also supported by American Cancer Society Grant RSG-12-053-01 (to D. A. C.).
[1] To whom correspondence should be addressed: Vascular Biology and Therapeutics Program, 10 Amistad St., New Haven, CT 06520. Tel.: 203-737-2214; Fax: 203-737-1484; E-mail: themis.kyriakides@yale.edu.

[2] The abbreviations used are: ECM, extracellular matrix; EC, endothelial cell; PAK, p21-activated kinase; GMFI, geometric mean fluorescence intensity; L-NAME, N^{ω}-nitro-L-arginine methyl ester hydrochloride; DKO, double knockout; eNOS, endothelial nitric-oxide synthase; tTG, tissue transglutaminase-2.

cells to migrate, adhere, and form functional protrusions guiding cell direction and velocity is essential (27).

Cell adhesion and migration are a reflection of proper signaling through Rho-GTPase family members, such as Rho, Rac, and Cdc42, which mediate actin cytoskeleton rearrangement in stress fiber, lamellipodia, and filipodia formation, and can be activated downstream of integrins (27–32). Reduced integrin signaling results in defects in cell adhesion, migration, and morphology (27, 33–36). Previous reports indicate that Akt1 KO mouse lung endothelial cells express similar surface levels of β1 and β3 integrins by Western blot (33); however, Akt1 is known to influence integrin signaling (27, 37), primarily through reduced signaling via Rac1 and p21-activated kinase (PAK) (27, 38). Rac1 function is dependent upon its location in the cell (27, 39–43), and Akt1 is known to regulate localization of Rac1 to lamellipodia to augment membrane ruffling during directional migration (27, 38). TSP2 expression has not been characterized in Akt1 KO fibroblasts, although their opposing effects on cell function indicate that their expression might be inversely related.

Injury- and ischemia-induced angiogenesis requires the production and utilization of endothelial nitric oxide synthase (eNOS)-derived nitric oxide (NO) that is synthesized downstream of Akt1 activation (44–46). NO is essential in maintaining vascular homeostasis by regulating tone, cell growth, and survival and providing protection from injury by modulating the angiogenic response (44, 47, 48). Akt1 KO mice, defective in NO production, exhibited impaired wound healing consistent with reduced angiogenesis as well as defective response to ischemia characterized by reduced blood flow recovery and reduced capillary/muscle fiber ratio (11, 49). These phenotypes were rescued using Akt1 KO mice with a knock-in mutation of eNOS mimicking constitutive activation (S1176D) but not with a loss of function eNOS mutation (S1176A) (49). Interestingly, high TSP2 expression accompanied low eNOS activation associated with the loss of Akt, and the converse was also true (10). In addition, the defective angiogenic phenotype in eNOS KO mice was rescued following the deletion of TSP2 (10). These observations indicate that the increased expression of TSP2 when NO levels are low contributes to the compromised healing phenotype and provide evidence for the physiological importance of TSP2 as a downstream target of Akt1-activated NO production.

When eNOS activation is low, as in Akt1 KO endothelial cells, survival, migration, adhesion, and proliferation are negatively affected (11, 27, 33, 37, 50, 51). In the current study, we show that Akt1-null primary dermal fibroblasts, which do not express eNOS or display NOS activity (52, 53), display increased levels of TSP2, suggesting an eNOS-independent regulation of TSP2 by Akt1. In contrast, it has been reported that Akt1 KO mice displayed enhanced angiogenesis in a number of *in vivo* models associated with decreased levels of TSP1 and TSP2, a phenotype that could be corrected by re-expression of TSP1 and TSP2 (12). Therefore, it is still unclear whether the compromised tissue repair phenotype of Akt1 KO mice is associated with increased TSP2 expression and if altering levels of TSP2 in Akt1 KO can affect the outcome of tissue repair in the same way that it did in eNOS KO.

EXPERIMENTAL PROCEDURES

Animals—The generation of TSP2 KO mice (9) and Akt1 KO mice (54) was described previously. Akt1/TSP2 DKO animals, as well as their WT counterparts, were generated by breeding of homozygotes. All genotypes were confirmed by PCR analysis using ear DNA and Western blot analysis on tissues as described (26, 54). All experiments were approved by the Institutional Animal Care and Use Committee at Yale University.

Reagents—Akt2 siRNA was purchased from Cell Signaling Technologies. Purified TSP2 was produced by stable expression of mTSP2 plasmid (plasmid 12411; Addgene.org) in CHO cells and isolation from medium as described previously (55). Cells were transfected with TSP2 shRNA (100 nM; Thermo Scientific) or Akt2 siRNA (50 nM; Cell Signaling) using Lipofectamine 2000 reagent (Invitrogen) as described in the manufacturer's protocol. For cell migration and adhesion assays as well as to visualize cell morphology, the cells were fixed and stained with a differential quick stain kit (modified Giemsa; Polysciences) or with DAPI and Alexa 568-conjugated phalloidin (Invitrogen). 0.5-μm Transwell chambers (Corning Inc.) were used for transwell migration assays. Inserts as well as tissue culture plastic for use in other assays were coated with a 0.1% gelatin solution, fibronectin (0–100 μg/ml; Sigma), or collagen I (Purecol, 1 mg/ml; Advanced Biomatrix).

Wounds—Full-thickness excisional wounds were made on the dorsum of each mouse as described previously (19), with the exception that 100 mg/kg ketamine and 10 mg/kg xylazine was used for anesthesia. Briefly, 6-mm biopsy punches (Acuderm, Ft. Lauderdale, FL) were used to create two identical wounds on each mouse, producing a total of 10 wounds/time point/genotype. At each time point, mice were sacrificed, and wounds were harvested with an excess of 2 mm unwounded tissue.

Tissue Processing and Analysis—Excised wounds were fixed in 10% (v/v) zinc-buffered formalin (Z-fix; Anatech) and embedded in paraffin. 5-μm sections were cut and stained with H&E. Immunohistochemistry using an anti-TSP2 antibody was performed as described previously (18, 22, 26, 56). TSP2 KO tissues were used as a control for antibody specificity. The Vector ABC Elite kit (Vector Laboratories) was used to amplify the immune reaction based on peroxidase activity. Fluorescent staining for isolectin B4 were performed on tissues as described previously (49). All stains were visualized using a Nikon Eclipse 800 microscope equipped with fluorescence optics. Metamorph software (Molecular Devices) was used to quantify the relative intensity of the fluorescent stain or peroxidase activity.

Cell Culture and Transfections—Primary mouse dermal fibroblasts were isolated and maintained in DMEM (Invitrogen) supplemented with 10% (v/v) FBS, penicillin, amphotericin-B, and L-glutamine as described previously (10). Primary dermal fibroblasts were plated in 6-well plates and transfected with either Akt2 siRNA (50 nM; Cell Signaling), scrambled siRNA (50 nM), TSP2 shRNA (100 nM; Thermo Scientific), empty vector (pSHAG-MAGIC, 1 μg/well), Rac1 G12V (2 μg/well; Addgene), or GFP control (2 μg/well, Addgene) using Lipofectamine 2000 (Life Technologies). After overnight incubation, the wells were washed with PBS, and fresh medium was replaced. After 24 h, the cells were replated for functional assays

(migration and adhesion) or collected for Western blot analysis. All transfection experiments were conducted in antibiotic-free medium. For treatment with DETANONOate (1 mM; Alexis Biochemicals) and L-NAME (1 mM; Sigma-Aldrich), cells were switched to starve medium (DMEM + 0.5% FBS) once they achieved 80% confluence and were treated for 24 h.

Scratch Cell Migration Assay—Primary dermal fibroblasts were seeded onto 24-well tissue culture plates at a density of 2.5×10^4/well in complete medium and allowed to grow to 100% confluence. To control for proliferation, cultures were pretreated with 50 μM mitomycin C for 30 min. A scratch was created in each well using a 200-μl pipette tip. The wells were washed once with PBS to remove displaced cells, fixed, and stained with a differential quick stain kit at each time point. Wells were viewed using a Nikon Eclipse 800 light microscope. Values are expressed as the ratio of cells migrating into the area of the original scratch at each time point compared with the number of cells that fill the scratch at 100% confluence. All experiments were performed in triplicate. 10 images were taken per well, resulting in a total of 30 images/genotype. Experiments were repeated three times. Analyses of area and cell numbers were performed using ImageJ software provided by the National Institutes of Health.

Transwell Cell Migration Assay—Transwell chambers were coated with gelatin by placing 100 μl of 0.5% gelatin solution on top of the filter insert and 500 μl in the bottom of the well and left overnight at 4 °C. After 24 h, the chambers were washed with PBS and placed into wells containing 500 μl of either starvation medium (0.5% FBS) or medium containing chemoattractant (10% FBS). Cells were starved in starvation medium overnight. 100 μl of starvation medium containing 6×10^4 cells was added to the top of the filter. The cells were then allowed to migrate through the filter for 6 h. Upon completion, the tops of the filters were gently wiped with a cotton applicator, and the cells that migrated through were fixed and stained with a differential quick stain kit. The experiment was performed in triplicate. 10 images were taken per filter using a Nikon Eclipse 800 light microscope, resulting in a total of 30 images/genotype. The experiment was repeated three times. Cell counts were performed using ImageJ software.

Cell Adhesion Assay—Cell attachment was performed in 24-well tissue culture plates that were either uncoated or precoated with 200 μl of fibronectin (100 μg/ml) or collagen I (1 mg/ml). 2.5×10^4 cells were seeded into the wells and left to attach for 24 h. Cells were fixed and stained using a differential quick stain kit or DAPI/phalloidin to visualize the formation of stress fibers. To examine manganese-induced cell adhesion, a 96-well plate was coated with varying concentrations of fibronectin (0–24 μg/ml) and allowed to incubate for 2 h at room temperature. Wells were blocked for 1 h at room temperature using 10 mg/ml BSA in PBS that had been heat-denatured at 95 °C for 10 min. Trypsinized cells at a concentration of 20,000 cells/100 μl in 1 mg/ml BSA were then added to the wells and incubated at 37 °C for 1, 3, 6, 12, or 24 h. Experiments were performed in triplicate, using three samples per genotype. 10 images/well were taken using a Nikon Eclipse 800 light microscope, for a total of 30 images/genotype. Experiments were repeated three times. Cell counts were performed using ImageJ software.

Cell Morphology—Cells were plated onto tissue culture plastic and allowed to adhere for 24 h, fixed, and either stained with a differential quick stain kit or fluorescently stained using an antibody for anti-GFP (Invitrogen) and DAPI/phalloidin. All stains were visualized using a Nikon Eclipse 800 microscope equipped with fluorescence optics. Measurements for cell morphology were performed by tracing the outline of at least 20 individual cells in at least 10 separate images/condition using the freehand tool in ImageJ software. For each cell, an analysis of area, perimeter, and shape (circularity) was performed by selecting each parameter in the measurements options to be displayed as results.

Immunocytochemistry—Cells plated at a density of 20,000 cells/well of a 24-well plate were grown in culture for 24 h and fixed with 90% methanol, 3% formaldehyde, and 7% water. Fixed cells were permeabilized by incubation with 0.1% Triton X-100 in PBS for 10 min and blocked using 1% BSA in PBS for 1 h, both at room temperature with agitation. Focal adhesions were visualized using an anti-paxillin antibody (1:200 dilution; Cell Signaling). Rac1 localization was observed using an anti-Rac1 antibody (1:200 dilution; Millipore). GFP was detected using an anti-GFP antibody (1:200 dilution; Invitrogen). Secondary antibodies were fluorescently labeled (Pierce).

Assessment of β1 Integrin Expression and Activation—Primary dermal fibroblasts were trypsinized using 0.25% trypsin, resuspended in DMEM, and labeled for a flow cytometric assay using an LSRII flow cytometer (BD Biosciences) to measure total β1 integrin surface expression and to separately assess $\alpha5\beta1$ integrin activation by measuring the binding of a fibronectin fragment (FN9-11) as described previously (57). FN9-11 binding to active integrins was conducted in the absence or presence of the general integrin inhibitor EDTA. Total activated β1 integrins were measured in the presence of a mouse β1 integrin-activating antibody (clone 9EG7, BD Pharmingen). Also, total β1 integrin expression levels were measured in parallel by staining with anti-β1 (HMβ-1, biotin-conjugated; Biolegend) antibody. Bound FN9-11 and integrin expression were detected with allophycocyanin-conjugated streptavidin (Thermo Scientific). The activation index calculated for FN9-11 was defined as $(F - F_0)/(F_A - F_0)$, where F is the GMFI of FN9-11 binding, F_0 is the GMFI of FN9-11 binding in the presence of integrin inhibitors, and F_A is the GMFI of FN9-11 binding in the presence of 9EG7. The normalized β1 integrin expression levels for each genotype are the calculated ratios of total anti-β1 integrin signal to wild type signal. FACS data analysis was carried out using FlowJo analysis software, and statistical analysis using Student's t test was performed by GraphPad Prism software.

Rac Activation Assay—Pull-down of GTP-bound Rac was accomplished using a Rac1/Cdc42 activation assay kit (Millipore) as described by the supplier. The experiment was performed by incubating cell lysates with GST fusion protein containing the p21-binding domain of PAK-1 bound to glutathione-agarose for 1 h at 4 °C. The amount of GTP-bound Rac was examined by immunoblotting using a Rac1 monoclonal antibody (Clone 23A8; Millipore).

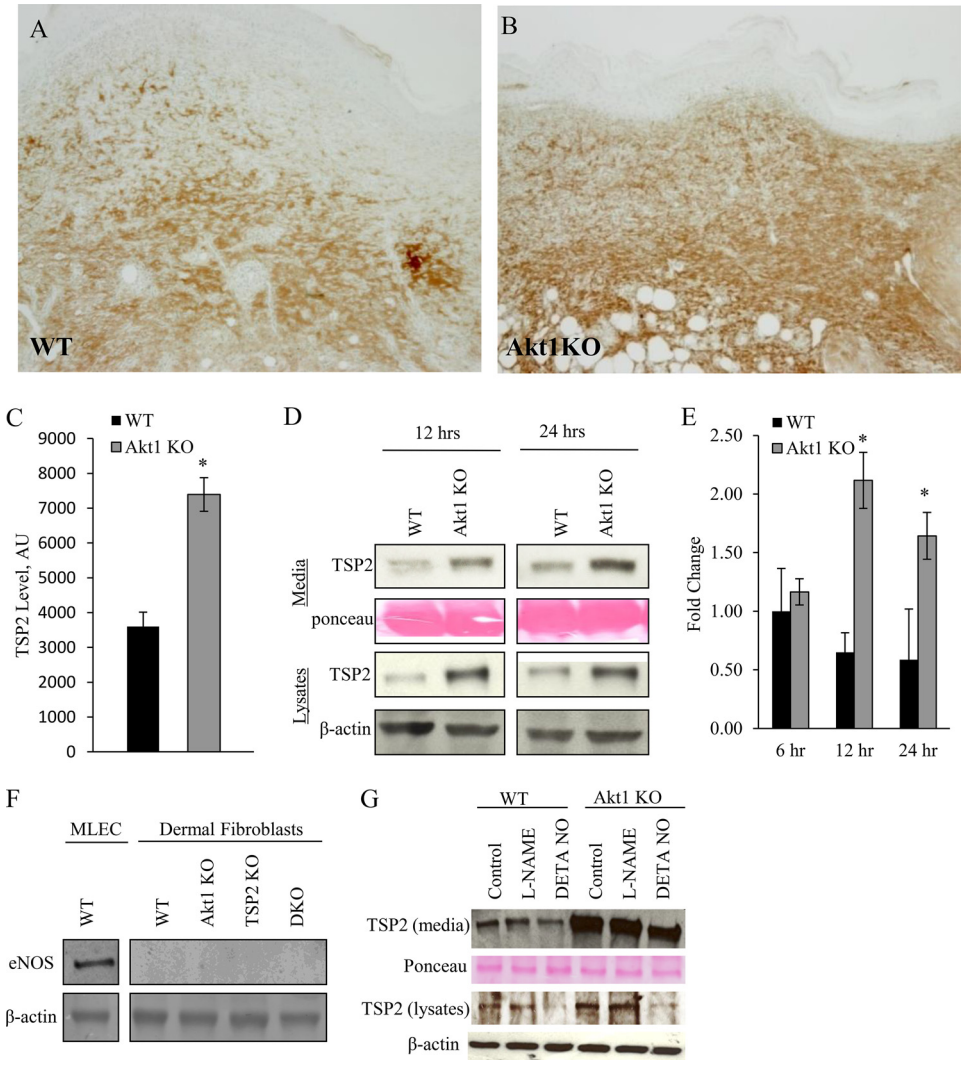

FIGURE 1. **Increased TSP2 in Akt1 KO tissues.** Representative images of day 10 dermal wounds from WT (*A*) and Akt1 KO (*B*) mice immunostained for TSP2 and visualized by the peroxidase reaction are shown (*brown*). Nuclei were counterstained with methylene green. Morphometric analysis revealed an increase in TSP2 deposition in Akt1 KO mice (*C*). Western blot analysis of conditioned medium and cell lysates shows increased TSP2 in Akt1 KO dermal fibroblasts at 12 and 24 h postplating (*D*). Quantitative PCR analysis shows increased TSP2 mRNA levels in Akt1 KO cells following a change in medium (*E*). Primary dermal fibroblasts isolated from all four genotypes do not express eNOS (*F*), and the regulation of TSP2 by Akt1 is not responsive to the NOS inhibitor L-NAME, but TSP2 levels can be reduced with the addition of an NO donor, DETANONOate (*G*). Data are expressed as the average ± S.E. (*error bars*). Original magnification was ×400 (*A*). *, $p \leq 0.05$.

Western Blotting—Cells growing in culture were lysed using radioimmune precipitation buffer supplemented with a protease inhibitor tablet (Roche Applied Science). Protein content of each sample was analyzed by a Bradford assay, as indicated by the supplier (Bio-Rad). A total of three samples per genotype were analyzed at each time point, and experiments were repeated in triplicate. Western blot analysis was performed using antibodies against TSP2 (1:250 dilution; BD Bioscience), β-actin (1:2000 dilution; Sigma), Akt1 (1:1000 dilution; Cell Signaling), Akt2 (1:1000 dilution; Cell Signaling), phospho-Akt Ser-473 (1:500 dilution; Cell Signaling), phosphogirdin (1:500; Abcam), eNOS (1:1000; Santa Cruz Biotechnology, Inc.), phospho- GSK3β (1:1000; Cell Signaling), phospho-S6K (1:500; Cell Signaling), and Akt (1:1000 dilution; Cell Signaling). Secondary antibodies were HRP-conjugated (Abcam).

Tissue Transglutaminase Activity Assay—Cells were plated at a density of 15,000 cells/well of a 96-well plate and allowed to grow for 24 h. After briefly washing the cultures in PBS, 5 mM $CaCl_2$, 3.85 mM dithiothreitol (DTT), and 0.1% biotin-cadaverine (Invitrogen) in reaction buffer (0.25 mM sucrose, 5 mM Tris-HCl (pH 7.4), and 2 mM EDTA (pH 7.4)) was added to the cells for 2 h at 37 °C. Subsequently, extravidin peroxidase (Sigma) diluted 1:5000 in 3% BSA blocking buffer was added for 1 h at 37 °C. Extravidin peroxidase activity was detected using tetramethylbenzidine.

Statistical Analysis—All data are represented as mean ± S.E. Student's *t* tests were performed, as indicated by the *bars* on each graph. Significance was defined as $p \leq 0.05$.

RESULTS

Increased TSP2 in Akt1 KO Tissues—Immunohistochemical detection of TSP2 in full-thickness day 10 dermal wounds revealed enhanced TSP2 deposition in ECM and fibroblasts in Akt1 KO animals (Fig. 1, *A* and *B*), which was quantified using

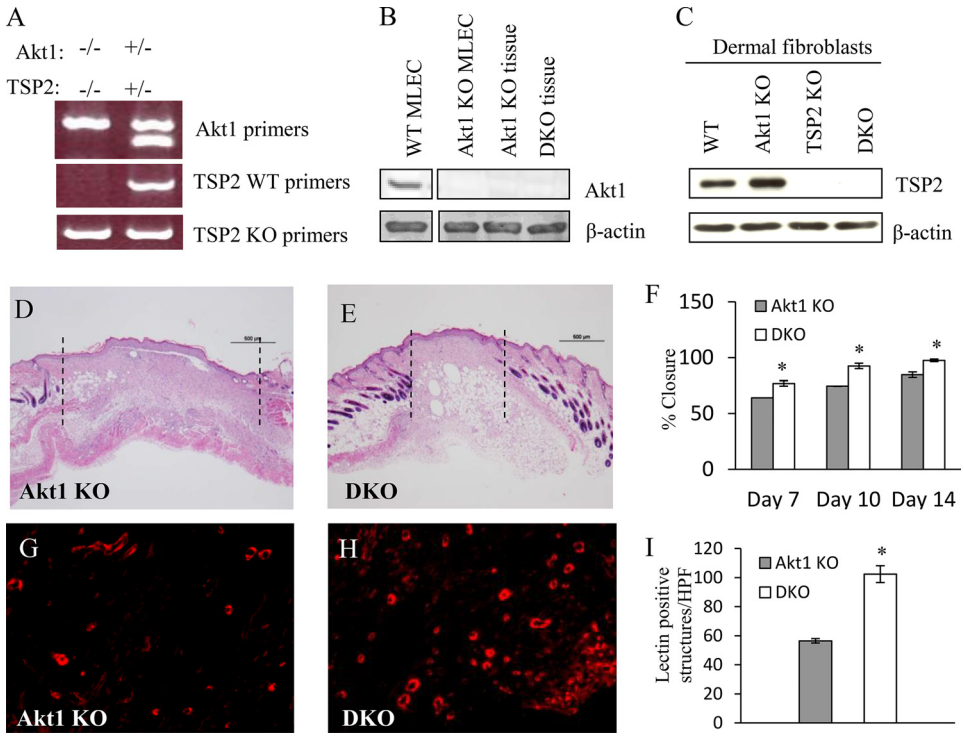

FIGURE 2. **Improved tissue repair in Akt1/TSP2 DKO mice.** *A*, Akt1/TSP2 double knock-out mice were genotyped by PCR using primers specific for WT, TSP2 KO, and Akt1 KO gene sequences. Western blot analysis of dermal fibroblast lysates and tissues confirmed the lack of Akt1 (*B*) and TSP2 (*C*) expression. Representative images of H&E-stained sections from day 10 wounds in Akt1 KO and DKO mice are shown (*D* and *E*). Wound closure, measured as the distance between the wound margins (as indicated by the *dotted lines* in *A*) was expressed as percentage closure and was greater in the DKO (*F*). Immunohistochemical detection of isolectin-B4 (*G* and *H*), revealed increased vessel formation in the DKO wounds. *I*, morphometric quantification of IB4 stains confirmed the increase in the DKO (original magnification, ×40 (*A*) and ×400 (*B*)). Data are expressed as the average ± S.E. (*error bars*). *, $p \leq 0.05$.

ImageJ (Fig. 1*C*). As stated above, fibroblasts are the primary producers of TSP2, and because they do not display intrinsic NOS activity, they permit the examination of TSP2 expression independent of eNOS. Western blot analysis revealed that primary dermal fibroblasts isolated from Akt1 KO mice had increased TSP2, both secreted into the medium and in cell lysates, when compared with WT as early as 12 h following a medium change (Fig. 1*D*). Moreover, quantitative RT-PCR analysis showed increased TSP2 mRNA levels in Akt1 KO cells (Fig. 1*E*) were significant at 12 and 24 h after changing medium in culture.

TSP2 Is Regulated by Akt1 in an eNOS-independent Manner in Dermal Fibroblasts—Previous reports confirm that dermal fibroblasts do not display intrinsic NOS activity; however, to determine whether primary cells were contaminated with a population of vascular cells during isolation, eNOS expression was evaluated by Western blot (Fig. 1*F*). Primary dermal fibroblasts do not express eNOS in the four genotypes we studied (WT, Akt1 KO, TSP2 KO, and DKO). Furthermore, when WT and Akt1 KO fibroblasts were treated with the NOS inhibitor L-NAME, there was no change in TSP2 protein levels by Western blot (Fig. 1*G*). However, treatment with the NO donor DETANONOate led to a reduction in the levels of TSP2 in both WT and Akt1 KO cells, suggesting that the negative regulation of TSP2 by NO is downstream of the effects of Akt1 on TSP2.

Improved Tissue Repair in Akt1/TSP2 DKO Mice—The preceding results establish that Akt1 knockout results in increased TSP2 expression. To elucidate the contribution of this increased TSP2 deposition to the impaired tissue repair observed in Akt1 KO mice, we generated Akt1/TSP2 DKO mice. Loss of both Akt1 and TSP2 were confirmed by PCR analysis of tail DNA (Fig. 2*A*) as well as protein lysates from primary cells and skin tissue by Western blotting (Fig. 2, *B* and *C*). We and others showed previously that Akt1 KO and TSP2 KO mice healed at decelerated and accelerated rates, respectively, when compared with WT (10, 11, 19, 49, 56). DKO mice displayed improved tissue repair during wound healing, as evidenced by reduced distance between wound margins and increased wound closure at multiple time points when compared with Akt1 KO alone (Fig. 2, *D–F*). The improved wound healing in DKO mice was associated with enhanced angiogenesis, as quantified by isolectin-B4 staining (Fig. 2, *G–I*).

Akt1 KO Dermal Fibroblasts Exhibit Defects in Migration and Adhesion Formation That Are Rescued in Akt1/TSP2 DKO Cells—To gain an understanding of the wound healing defect, we analyzed fibroblasts in a scratch migration assay. Akt1 KO fibroblasts were impaired in their ability to migrate (Fig. 3*A*). A transwell migration assay using serum as a chemoattractant further validated this defect (Fig. 3*B*). In contrast, DKO primary dermal fibroblasts displayed migration rates similar to that of WT cells (Fig. 3, *A* and *B*), suggesting that elevated TSP2 levels contribute to impaired cell migration in Akt1 KO cells. Additionally, Akt1 KO cells assumed a rounded morphology, a defect that was improved in the DKO cells (Fig. 3*C*). Stress fiber formation was diminished in Akt1 KO cells, whereas DKO cells displayed robust stress fibers similar to those in WT cells (Fig. 3, *D–G*). Additionally, focal adhesions were examined by immunostaining for paxillin (Fig. 3, *H–K*). Akt1 KO fibroblasts displayed both reduced total paxillin staining (Fig. 3*L*) and a reduc-

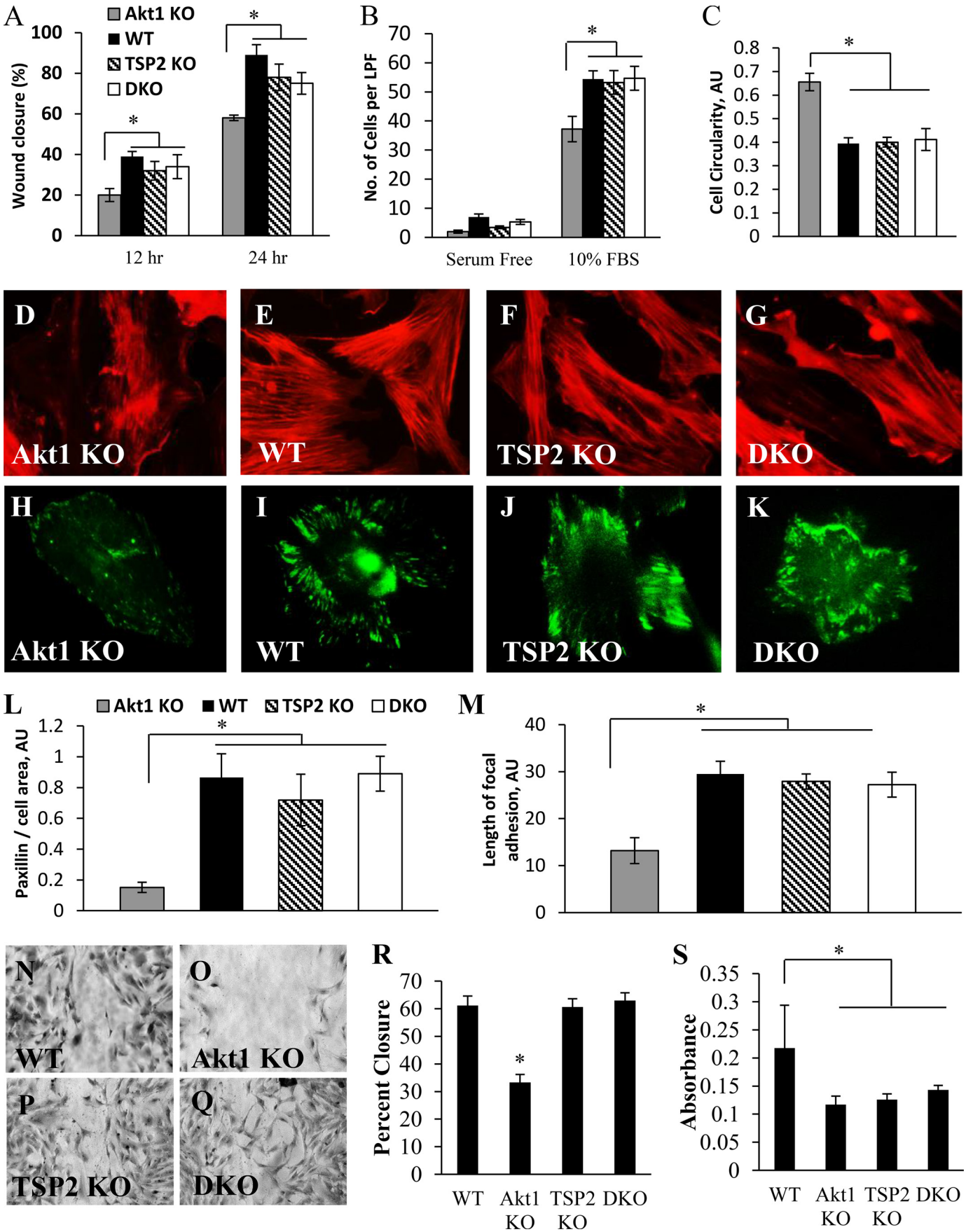
A
Akt1 KO
WT
TSP2 KO
DKO
Wound closure (%)
100
80
60
40
20
0
*
*
12 hr
24 hr
B
No. of Cells per LPF
70
60
50
40
30
20
10
0
*
Serum Free
10% FBS
C
Cell Circularity, AU
0.8
0.7
0.6
0.5
0.4
0.3
0.2
0.1
0
*
D
Akt1 KO
E
WT
F
TSP2 KO
G
DKO
H
Akt1 KO
I
WT
J
TSP2 KO
K
DKO
L
Akt1 KO
WT
TSP2 KO
DKO
Paxillin / cell area, AU
1.2
1
0.8
0.6
0.4
0.2
0
*
M
Length of focal adhesion, AU
40
30
20
10
0
*
N
WT
O
Akt1 KO
P
TSP2 KO
Q
DKO
R
Percent Closure
70
60
50
40
30
20
10
0
*
WT
Akt1 KO
TSP2 KO
DKO
S
Absorbance
0.35
0.3
0.25
0.2
0.15
0.1
0.05
0
*
WT
Akt1 KO
TSP2 KO
DKO

tion in the size of focal adhesions (Fig. 3*M*) when compared with WT, TSP2 KO, and DKO cells. Pretreatment with mitomycin C did not alter the migration defect, suggesting that this effect is independent of proliferation (Fig. 3, *N–R*) Together, these data suggest that knockout of Akt1 affects multiple cellular functions that are relevant to tissue repair and that loss of TSP2 in the Akt1 KO background is sufficient to rescue the observed cellular defects.

It was previously shown that TSP2 KO cells display reduced activity of tissue transglutaminase-2 (tTG), resulting in altered cell adhesion (58). To investigate the contribution of this mechanism to the adhesion defect of the Akt1 KO cells, the activity of tTG in WT, Akt1 KO, TSP2 KO, and DKO fibroblasts was measured using a biotin-cadaverine incorporation assay. Akt1 KO, TSP2 KO, and DKO fibroblasts displayed decreased tTG activity when compared with WT (Fig. 3*S*), suggesting that this mechanism is unrelated to the phenotype of Akt1 KO fibroblasts because the cell defects are rescued in DKO cells without restoring tTG activity levels. Additionally, treatment with the tTG inhibitor, cystamine (5 μM), abolished tTG activity in all genotypes studied but did not influence cell morphology or adhesion (not shown), confirming that changes in tTG activity are not a factor in the phenotype of Akt1 KO or DKO fibroblasts.

Compensation by Akt2 Does Not Regulate TSP2 Expression or Cellular Function—Recent evidence suggests that each of the three Akt isoforms fulfills distinct roles by phosphorylating specific targets (32, 59), including some that are shared between all isoforms. However, because of the importance of each isoform to cell survival, compensation from other isoforms when one is lost is not uncommon (60, 61). Fig. 4*A* shows persistent levels of phosphorylated Akt at serine 473 in Akt1 KO fibroblasts following a medium change concomitant with an increase in Akt2 protein levels via Western blotting. This increase in Akt2 expression was confirmed at the transcriptional level by quantitative RT-PCR (Fig. 4*B*). Levels of Akt3 measured by quantitative RT-PCR in Akt1 KO dermal fibroblasts were found to be similar to that of WT (Fig. 4*C*), indicating that the compensation is specific to the Akt2 isoform.

However, knockdown of Akt2 did not change the levels of secreted or intracellular TSP2 (Fig. 4*D*). Migration rates were unaffected by Akt2 knockdown in WT (Fig. 4*E*) as well as in Akt1 KO cells (Fig. 4*F*). Together, these data suggest that there are Akt1-dependent events regulating TSP2 production and cellular functions that are not rescued by compensation from Akt2.

TSP2 has been previously shown to modulate Akt by inhibiting VEGF-mediated EC growth signals (55). Therefore, we investigated whether TSP2 influences Akt2 levels by inducing an Akt1 KO-like state. Indeed, the addition of TSP2 to WT fibroblasts increases Akt2 (Fig. 4*G*), suggesting that increased TSP2 may contribute to compensation by Akt2 when Akt1 is lost.

We next investigated whether compensation from Akt2 contributed to the phosphorylation of key Akt substrates involved in cell motility. Phosphorylation of girdin at serine-1416 by Akt promotes cell motility by regulating actin filament integrity at the leading edge of migrating cells. Akt1 KO cells display reduced phospho-girdin levels by Western blot, which is not rescued in DKO cells (Fig. 4*H*). TSP2 KO and WT fibroblasts display comparable levels of phospho-girdin, indicating that TSP2 does not modulate its phosphorylation. Together, these data indicate that the loss of TSP2 is affecting a pathway independent of girdin to regulate cell motility. Other pathways, such as those mediated by p70 S6 kinase and GSK-3β, were not influenced by the loss of Akt1, suggesting that they are controlled redundantly among the isoforms and are maintained by Akt2 compensation in Akt1 KO cells.

TSP2 Expression in Akt1 KO Dermal Fibroblasts Is Essential for Cell Defects—WT fibroblasts treated with exogenous, recombinant TSP2 displayed altered cell morphology and reduced adhesion comparable with that of Akt1 KO fibroblasts (Fig. 5, *A*, *B*, and *E*). Conversely, knockdown of TSP2 in Akt1 KO fibroblasts resulted in an increase in cell spreading and adhesion comparable with WT levels (Fig. 5, *C–E*). Additionally, treatment with exogenous TSP2 resulted in reduced migration rates in WT fibroblasts, whereas knockdown of TSP2 improved migration rates in Akt1 KO fibroblasts (Fig. 5*F*), suggesting that TSP2 levels are responsible for the cellular defects in Akt1 KO dermal fibroblasts and that changes in the level of TSP2 are sufficient to rescue this phenotype. Sufficient knockdown of TSP2 expression was verified by Western blotting (Fig. 5*G*).

Collagen I and Fibronectin Influence Akt1 KO Cell Morphology and Adhesion Independent of β1 Integrin Activation—To further probe the morphological defects of Akt1 KO fibroblasts, these cells were plated on either collagen I- or fibronectin-coated substrates. Akt1 KO fibroblasts displayed normal morphology and density when plated for 24 h on fibronectin-coated but not collagen type 1-coated surfaces (Fig. 6), suggesting that high concentrations of fibronectin can compensate for the observed defects. We next sought to investigate integrin-mediated adhesion by stimulating cells with manganese (Mn^{2+}; 1 mM) to activate integrins because Akt1 is known to influence integrin signaling (37). After 1 h of plating, Akt1 KO fibroblasts displayed an adhesion defect that was not rescued by treatment with Mn^{2+} (Fig. 7*A*), suggesting that the effect may not be due to defects in integrin activation. However, this observation does not rule out effects due to surface expression of integrins or integrin clustering effects that would influence downstream

FIGURE 3. **Increased TSP2 expression in Akt1 KO dermal fibroblasts contributes to functional defects.** Scratch (*A*) and transwell (*B*) migration assays revealed that Akt1 KO fibroblasts were impaired in migration, and this defect was not evident in DKO fibroblasts. *C*, image analysis of revealed increased circularity of Akt1 KO fibroblasts. *D–G*, representative images of cell stained with rhodamine-phalloidin to visualize stress fiber are shown. *H–K*, representative images of cells stained with paxillin to visualize focal adhesions. Image analysis revealed reduced paxillin (*L*) and reduced focal adhesion length (*M*) in Akt1 KO cells. Inhibition of proliferation with pretreatment with mitomycin C (50 μM) resulted in persistence of the migration defect of Akt1 KO fibroblasts. Representative phase-contrast images of cells 24 h after scratching revealed reduced migration in Akt1 KO cells (*O*) when compared with WT (*N*), TSP2 KO (*P*), and DKO (*Q*), which was quantified in *R*. Reduced tTG activity in Akt1 KO cells is not rescued in DKO fibroblasts. A biotin-cadaverine incorporation assay revealed reduced tTG activity in Akt1 KO, TSP2 KO, and DKO fibroblasts when compared with WT (*S*). *LPF*, low power field; *AU*, arbitrary units. Original magnification was ×100 (*D*), ×400 (*E* and *F*), and ×200 (*N–Q*). Data are expressed as the average ± S.E. (*error bars*) *, $p \leq 0.05$.

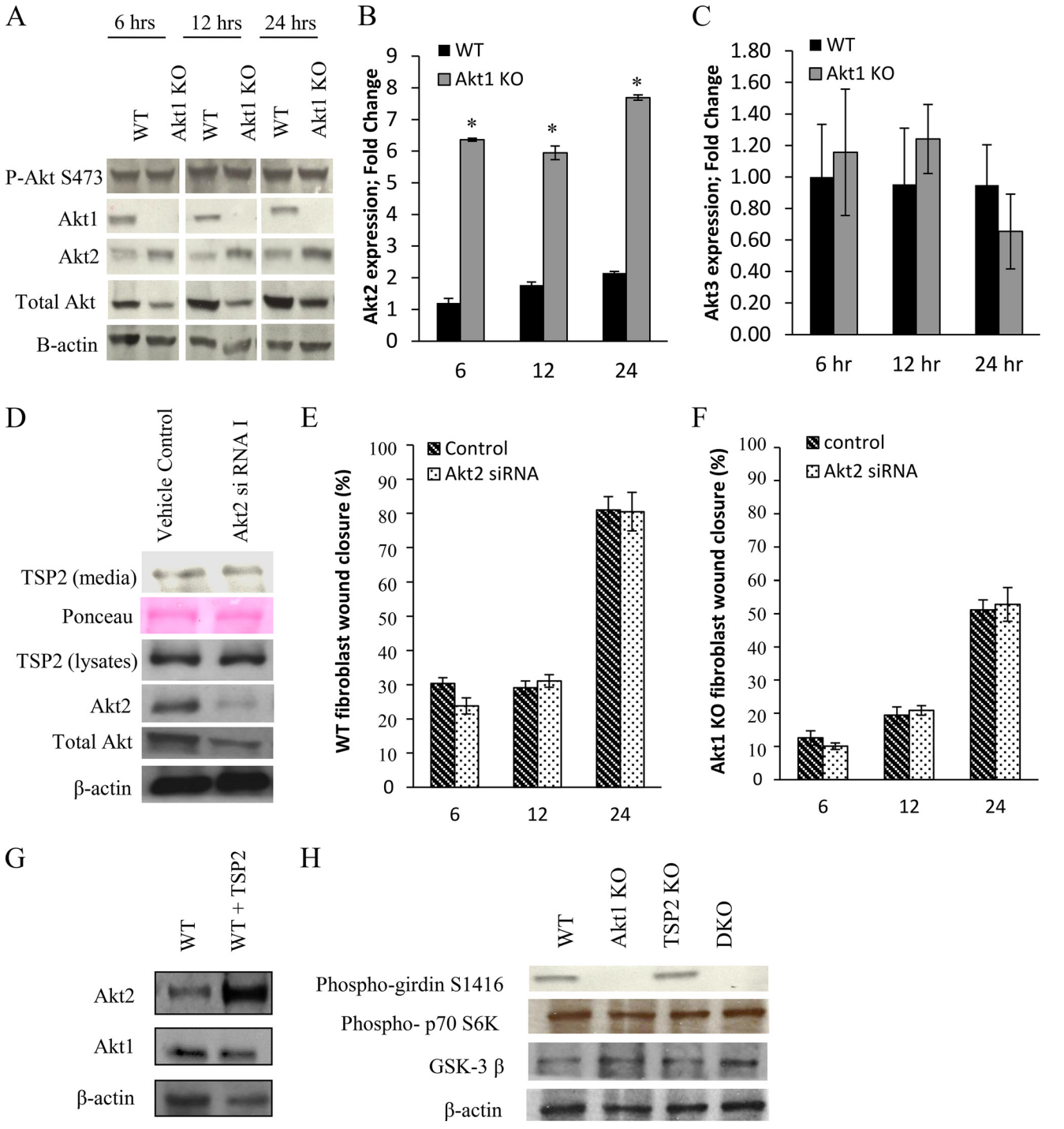

FIGURE 4. **Compensation by Akt2 does not regulate TSP2 expression or cellular function.** *A*, Western blot analysis of lysates from WT and Akt1 KO fibroblasts show persistent levels of phospho-Akt at serine 473 in Akt1 KO cells following a medium change, despite the complete loss of the Akt1 isoform. Both Western blot (*A*) and quantitative PCR (*B*) analysis reveal an increase in expression of Akt2 in Akt1 KO cells. *C*, quantitative PCR analysis revealed no changes in Akt3 mRNA expression in Akt1 KO cells. Akt2-specific siRNA knocked down Akt2 expression in WT fibroblasts but did not affect TSP2 expression (*D*). Akt2 knockdown in WT or Akt1 KO cells did not influence migration. *E* and *F*, the addition of TSP2 to WT fibroblast resulted in an increase in Akt2 protein by Western blot (*G*). Compensation by Akt2 in Akt1 KO fibroblasts was not sufficient to maintain levels of phosphogirdin but contributed to p70S6K and GSK-3β signaling (*H*). Data are expressed as the average ± S.E. (*error bars*). *, $p \leq 0.05$.

signaling. FACS analysis of β1 integrin surface expression (Fig. 7*B*) and activation (Fig. 7*C*) in non-permeabilized primary dermal fibroblasts did not reveal significant differences among all four genotypes examined. The observed defects were consistent with reduced integrin signaling (27, 33–36); therefore, we investigated the effect of reduced or delayed integrin signaling by examining fibroblast adhesion to various concentrations of fibronectin over the course of 24 h (Fig. 7, *D–F*). At low (1.5 μg/ml) and intermediate (12 μg/ml) fibronectin coating concentrations, the Akt1 KO cells exhibited adhesion defects at all time points tested, whereas DKO cells behaved like WT cells. The adhesive defect of the Akt1 KO cells was only restored at

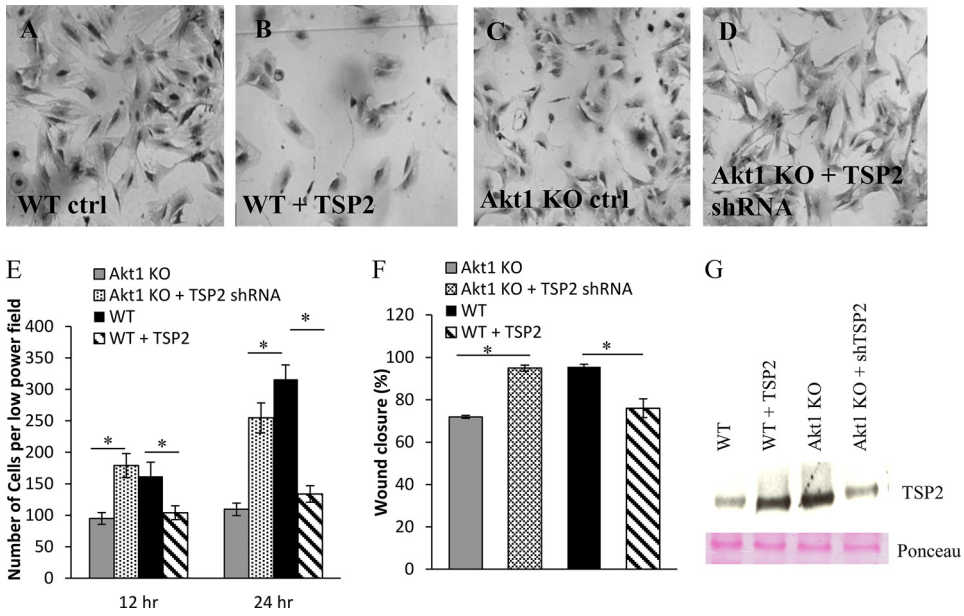

FIGURE 5. **TSP2 expression in Akt1 KO dermal fibroblasts contributes to cell defects.** Representative phase-contrast images show that knockdown of TSP2 in Akt1 KO or the addition of exogenous TSP2 to WT cells resulted in changes in cell morphology (*A–D*). Quantification of scratch wound closure and adhesion after 24 h showed increased and reduced migration in Akt1 KO cells with knockdown TSP2 and WT cells treated with exogenous TSP2, respectively (*E* and *F*). *G*, changes in TSP2 levels following shRNA knockdown or the addition of TSP2 were confirmed by Western blot of conditioned media. Data are expressed as the average ± S.E. (*error bars*); $p \leq 0.05$. Original magnification was ×200 (*A* and *B*).

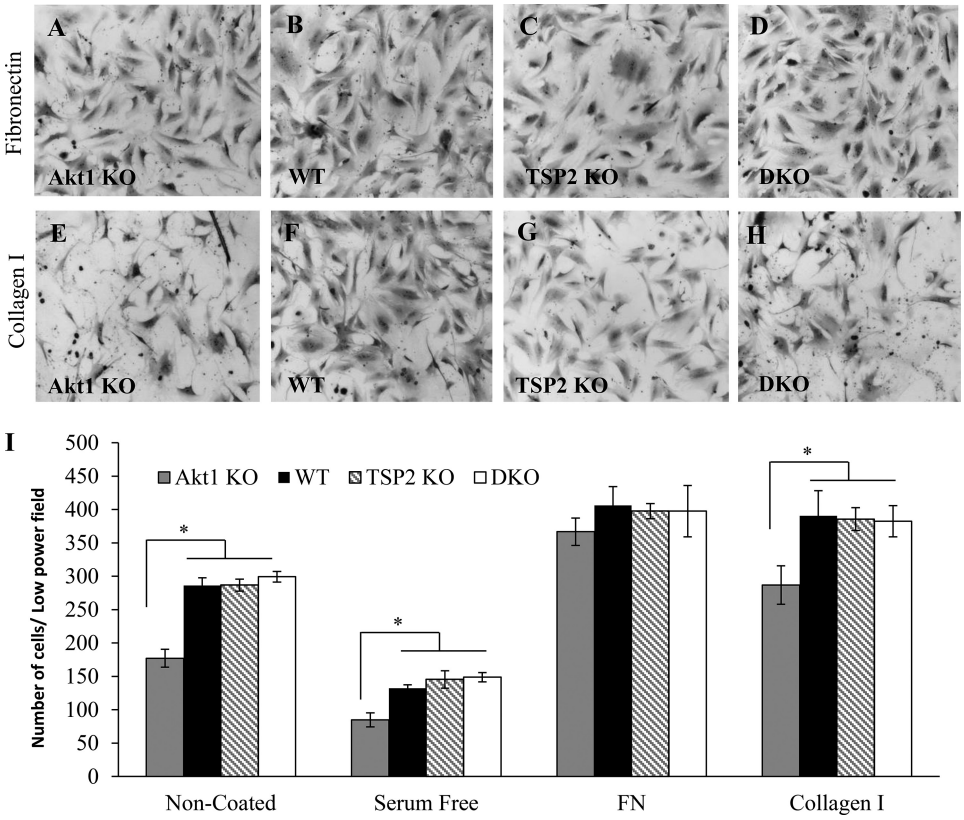

FIGURE 6. **Fibronectin rescues defects in Akt1 KO cell morphology and adhesion.** Representative phase-contrast images of cells plated for 24 h on fibronectin-coated (*A–D*) or collagen I-coated (*E–H*) wells are shown. Akt1 KO fibroblasts displayed normal morphology only in fibronectin-coated wells (*A*). *I*, adhesion of Akt1 KO fibroblasts was normal on fibronectin (*FN*)-coated surfaces. Data are expressed as the average ± S.E. (*error bars*) *, $p \leq 0.05$. Original magnification was ×200 (*A–H*).

late time points (24 h) on a high concentration of fibronectin (24 μg/ml; Fig. 7*F*), suggesting a defect in post occupancy signaling that can be compensated by very high fibronectin concentrations. This defect is not specific for fibronectin as opposed to collagen I because the defect is evident at low concentrations of fibronectin at early time points. Together, these

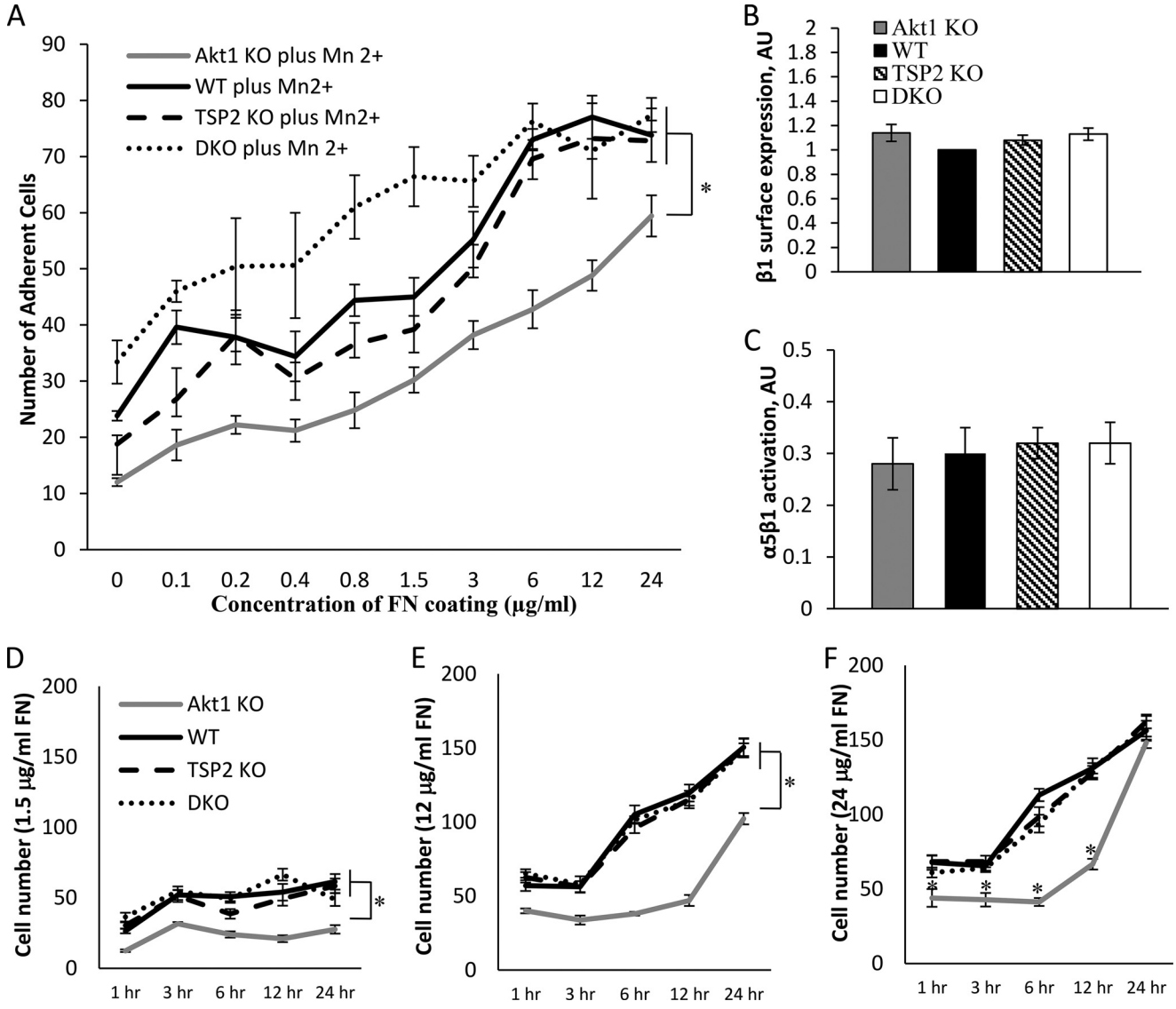

FIGURE 7. **Akt1 KO cell adhesion is impaired independently of β1 integrin expression and activation.** *A*, cell adhesion on various concentrations of fibronectin-coated wells in the presence or absence of Mn^{2+} was measured at 1 h. The adhesion defect of Akt1 KO fibroblasts did not improve by the addition of Mn^{2+} on the highest concentration of fibronectin (*FN*). In contrast, DKO fibroblasts displayed increased adhesion. *B*, β1 integrin surface expression was similar in all cell types. In addition, the ratios of active α5β1 integrin (measured by FN9-11) to total β1 integrin levels were equal in all cell types (*C*). *D–F*, cells were allowed to adhere to 1.5, 12, or 24 µg/ml fibronectin-coated wells, and adhesion was measured at 1, 3, 6, 12, and 24 h. Akt1 KO cells displayed improved adhesion only at 24 h at the highest concentration of fibronectin (24 µg/ml). *AU*, arbitrary units. Data are expressed as the average ± S.E. (*error bars*). *, $p \leq 0.05$.

data suggest that there may be more α5 than α2 integrin present on the cells, so collagen never reaches a high enough occupancy to overcome the deficit.

Consistent with this suggestion, we observed that the absence of Akt1 resulted in a significant reduction of Rac1 activity under basal conditions, assayed as Rac1-GTP (Fig. 8*A*). This was dependent upon the presence of TSP2 because DKO dermal fibroblasts displayed increased Rac1 activity, and the addition of exogenous TSP2 to the medium of DKO fibroblasts grown in culture diminished this effect. Consistent with previous reports and Fig. 8*A*, we observed increased cytoplasmic Rac1 localization in Akt1 KO fibroblasts, suggesting reduced Rac1-PAK signaling (Fig. 8, *C–F*). WT, TSP2, and DKO fibroblasts displayed increased membrane and lamellipodia localization of Rac1, which correlated with elevated Rac1 activity shown in Fig. 8*A*. Moreover, expression of a Rac point mutant deficient in GTPase activity, rendering it constitutively active (G12V), resulted in increased spreading in WT fibroblasts (Fig. 8, *G–J*). Consistent with Fig. 3, Akt1 KO fibroblasts displayed a rounded cell morphology (Fig. 8, *K* and *L*), but this defect was rescued by expression of the G12V mutant (Fig. 8, *M* and *N*). Consistent with Fig. 5*B*, WT fibroblasts treated with exogenous TSP2 exhibited a rounded morphology similar to that of Akt1 KO cells (Fig. 8, *O* and *P*) that was also rescued by expression of Rac G12V (Fig. 8, *Q* and *R*).

Expression of the Rac G12V mutant resulted in similar cell area, perimeter, and circularity in WT, Akt1 KO, and WT fibroblasts treated with TSP2 (Fig. 8, *S–U*), signifying that the morphological defect caused by increased TSP2 expression is a result of reduced Rac-induced cell spreading. Together, these data suggest a direct regulation of Rac1 by TSP2 that results in compromised cell function in Akt1 KO cells.

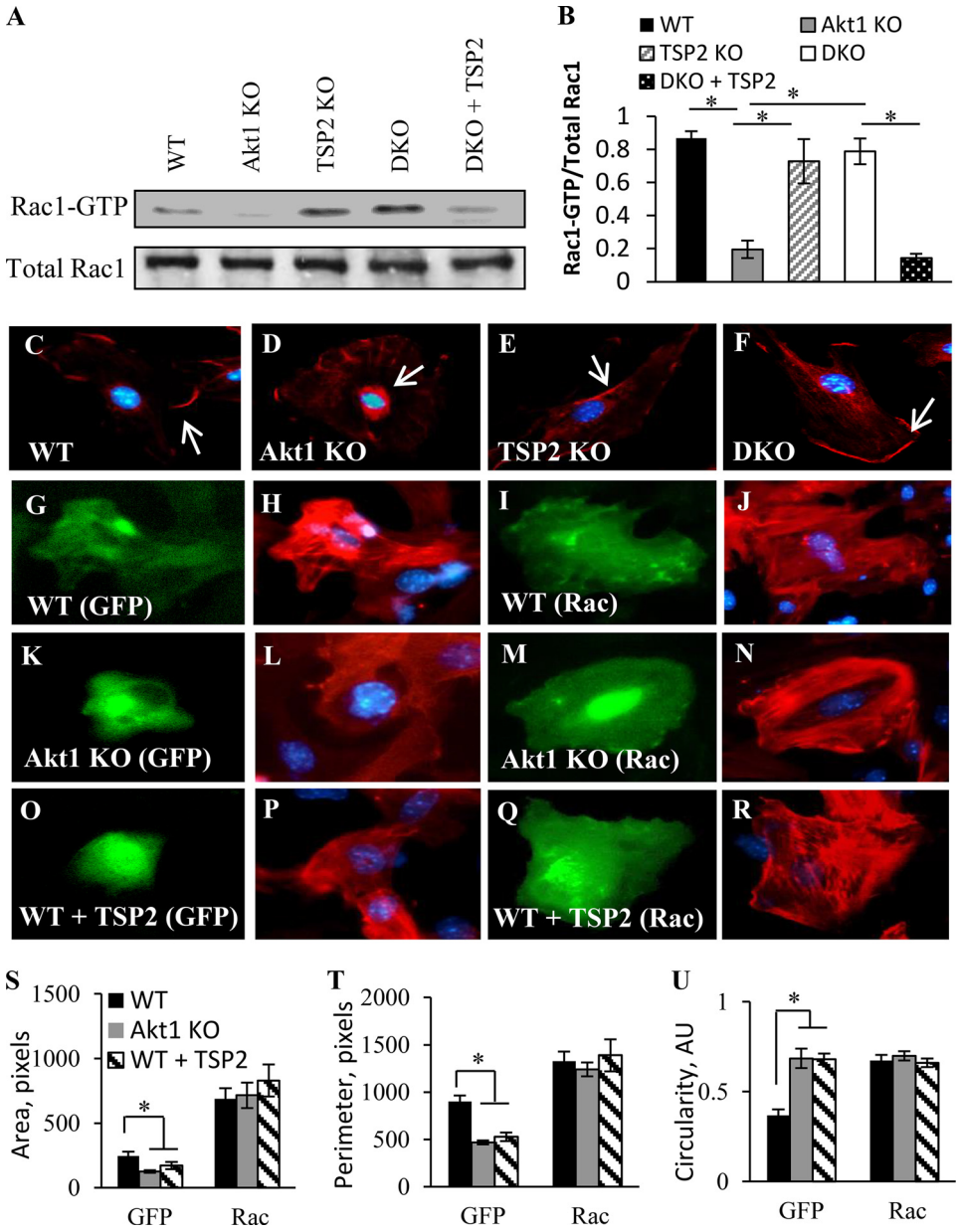

FIGURE 8. **Increased TSP2 regulates Rac1 activity in Akt1 KO fibroblasts.** *A*, pull-down assay of active Rac1 in fibroblasts shows reduced levels in Akt1 KO fibroblasts and DKO fibroblasts treated with exogenous TSP2. Active Rac1 is shown as Rac1-GTP. *B*, Rac1 activity expressed as the ratio of active to total Rac1. *C–F*, immunofluorescent detection of Rac1 showed predominant cytoplasmic localization in Akt1 KO fibroblasts. *Arrows* in the images show membrane-associated Rac1. Representative images are shown of WT (*G–J*) and Akt1 KO fibroblasts (*K–N*) as well as WT fibroblasts treated with TSP2 (*O–R*) transfected with GFP (*left panels*) or Rac G12V-GFP (*right panels*). Constitutively active Rac G12V rescues the morphological defects of Akt1 KO fibroblasts and WT fibroblasts treated with TSP2 (*N* and *R*), as demonstrated by rhodamine-phalloidin staining. This rescue resulted in cell area (*S*), perimeter (*T*), and circularity (*U*) values similar to WT fibroblasts. Nuclei were counterstained with DAPI. Data are expressed as the average ± S.E. (*error bars*) *, $p \leq 0.05$. Original magnification was ×400 (*C*).

DISCUSSION

The central finding of this paper is that the loss of Akt1 results in increased TSP2 levels, which contributes to delayed wound healing of Akt1 knock-out mice. Results showing that Akt1/TSP2 DKO mice exhibit accelerated wound healing compared with Akt1 KO support this conclusion. Mechanistically, fibroblasts from Akt1 KO mice have elevated TSP2 levels and are impaired in wound closure, migration, and adhesion *in vitro*. Elimination of TSP2 genetically or via shRNA rescues these phenotypes. The loss of Akt1 and elevation of TSP2 impairs Rac1 activation in fibroblasts, an effect rescued by the addition of recombinant TSP2. Collectively, these data support a model by which Akt1 regulation of TSP2 is critical for matricellular communication and cell morphogenesis.

Akt has been well characterized as an essential component of postnatal angiogenesis following injury by phosphorylating many substrates, one of which is eNOS, which gives rise to NO. Similar to the Akt1 KO mice, eNOS KO mice are impaired in their ability to heal efficiently following dermal wounding and hind limb ischemia (47, 48). In fact, Akt1 regulates postinjury angiogenesis largely through activation of eNOS because mice carrying a knock-in mutation (serine to aspartate substitution)

of the critical Akt1 phosphorylation site on eNOS (serine 1176) that renders the enzyme constitutively active display improved wound healing and recovery from hind limb ischemia (49). Our data showing increased TSP2 in Akt1 KO tissues are consistent with previous findings associating defective healing with increased levels of TSP2, such as in aged mice and eNOS KO mice (10, 20). Part of this increased expression level can be attributed to the negative regulation of TSP2 by NO. Indeed, rendering eNOS constitutively active in the Akt1 KO mice results in reduced TSP2 expression (10). However, because TSP2 levels are elevated in primary dermal fibroblasts that do not express eNOS, our data support a novel, NO-independent TSP2 regulatory mechanism.

Elevated TSP2 levels found in Akt1 KO mice stand in contrast to a previous report showing decreased TSP1 and TSP2 levels in melanoma tumors implanted into Akt1 KO mice (12). Specifically, increased TSP1 expression in endothelial cells with transfection of myristoylated Akt and reduced TSP1 expression by transfection of dominant-negative Akt were reported. However, the direct effect of Akt1 on TSP1 or TSP2 levels or whether NO was a component of the regulation was not discussed. More importantly, it was indicated that there was only a small decrease in NO production in the Akt1 KO mice used in the study, which differs from previous reports in the mice used in the present study, where a marked reduction in eNOS activation and NO production was found (49). Therefore, differences in mouse strains, compensation by other Akt isoforms, and the relative contribution of NO levels to the observed processes may explain these conflicting *in vivo* observations. In addition, a later study reported impaired wound healing, associated with impaired angiogenesis, in Akt1 KO mice (12, 62), but the levels of TSP1 or TSP2 were not analyzed.

Akt1 KO cells were previously described to display impaired β1 integrin activation and defects in Rac1-PAK signaling, resulting in reduced cell adhesion and migration (27, 33, 38, 63). Although we did not observe changes in β1 integrin expression or activation in primary dermal fibroblasts by FACS analysis, it is possible that the effect of Akt1 on integrin expression and activation is sensitive to subtle differences in mouse strains, such as in isoform compensation. Each of the three Akt isoforms can phosphorylate distinct targets; however, when faced with the loss of one isoform, cells compensate by increasing the expression of other isoforms or AGC kinases to increase signaling through redundant targets and increase cell survival (32, 60, 61).

Reports indicate that Akt1 influences integrin signaling via Rac1-PAK; however, our data suggest that this effect is mediated, at least in part, by the altered expression levels of TSP2. In the present study, we showed that Akt1 KO dermal fibroblasts, while expressing increased levels of TSP2, display defects in cell adhesion, migration, and morphology, all of which are consistent with reduced Rac1 activity. These molecular defects were rescued in the DKO cells and could be altered by manipulating TSP2 levels, indicating that TSP2 directly modulates Rac1-PAK signaling. Based on these observations, a new role for TSP2 in cytoskeletal rearrangement and morphology, cell attachment, and Rac1-PAK and integrin signaling is suggested. In addition, our data support a role for Akt in regulating cell-matrix interactions and matrix assembly following injury by influencing TSP2.

During wound healing, fibroblasts generate and remodel ECM in the connective tissue. In order to repair connective tissue, fibroblasts must migrate into the wound and attach to pre-existing ECM through focal adhesions, which mediate adhesion between the cell cytoskeleton and the surrounding matrix through integrins (64). Proper signaling through β1 integrin in fibroblasts is essential for normal wound healing *in vivo* because fibroblasts with reduced β1 expression display diminished cell adhesion (65). Moreover, fibroblasts that lack proper signaling through integrin receptors and Rac1-PAK assume a rounded morphology and adhere poorly to substrates. As a direct result, they cannot undergo fibrogenesis and cutaneous wound healing, suggesting that cell adhesion is a critical component of normal tissue repair to allow cells to migrate (18, 31, 66–71). Consistent with these findings, our *in vitro* data suggest that diminished Rac1 activation results in compromised fibroblast function, which could also contribute to the compromised wound healing in Akt1 KO mice. Rac1 activation is restored in DKO fibroblasts, leading to improved fibroblast adhesion and migration, and as a result, tissue repair is greatly enhanced in these mice.

Akt1 is a pro-angiogenic, signaling kinase that is necessary for proper healing, and Akt signaling results in increased functional vasculature in a wound bed. Previously, NO was shown to contribute to angiogenesis by promoting blood flow, cell growth, cell migration, and EC survival, and the present data demonstrate that tissue repair and angiogenesis can be rescued in Akt1 KO mice by the loss of TSP2, suggesting that regulation of TSP2 is an essential function of Akt1. Furthermore, alteration of TSP2 levels alone is sufficient to rescue defective wound angiogenesis in the Akt1 KO mice. These data, in conjunction with previous data showing that eNOS-derived NO can regulate TSP2 levels in EC (10), suggest that Akt1 can determine the levels of TSP2 in a cell type-specific manner to integrate responses of EC and fibroblasts, two cell types crucial for proper wound healing.

Acknowledgment—We thank Annarita DiLorenzo for technical assistance with animal breeding.

REFERENCES

1. Folkman, J. (2003) Fundamental concepts of the angiogenic process. *Curr. Mol. Med.* **3,** 643–651
2. Folkman, J., and Klagsbrun, M. (1987) Angiogenic factors. *Science* **235,** 442–447
3. Skaletz-Rorowski, A., Kureishi, Y., Shiojima, I., and Walsh, K. (2004) The pro- and antiangiogenic effects of statins. *Semin. Vasc. Med.* **4,** 395–400
4. Adya, R., Tan, B. K., Chen, J., and Randeva, H. S. (2012) Protective actions of globular and full-length adiponectin on human endothelial cells: novel insights into adiponectin-induced angiogenesis. *J. Vasc. Res.* **49,** 534–543
5. Zachary, I., and Gliki, G. (2001) Signaling transduction mechanisms mediating biological actions of the vascular endothelial growth factor family. *Cardiovasc. Res.* **49,** 568–581
6. Sessa, W. C. (2009) Molecular control of blood flow and angiogenesis: role of nitric oxide. *J. Thromb. Haemost.* **7,** 35–37
7. Suárez, Y., and Sessa, W. C. (2009) MicroRNAs as novel regulators of angiogenesis. *Circ. Res.* **104,** 442–454
8. Carmeliet, P., and Jain, R. K. (2011) Molecular mechanisms and clinical

applications of angiogenesis. *Nature* **473,** 298–307
9. Kyriakides, T. R., Zhu, Y. H., Yang, Z., and Bornstein, P. (1998) The distribution of the matricellular protein thrombospondin 2 in tissues of embryonic and adult mice. *J. Histochem. Cytochem.* **46,** 1007–1015
10. MacLauchlan, S., Yu, J., Parrish, M., Asoulin, T. A., Schleicher, M., Krady, M. M., Zeng, J., Huang, P. L., Sessa, W. C., and Kyriakides, T. R. (2011) Endothelial nitric oxide synthase controls the expression of the angiogenesis inhibitor thrombospondin 2. *Proc. Natl. Acad. Sci. U.S.A.* **108,** E1137–E1145
11. Ackah, E., Yu, J., Zoellner, S., Iwakiri, Y., Skurk, C., Shibata, R., Ouchi, N., Easton, R. M., Galasso, G., Birnbaum, M. J., Walsh, K., and Sessa, W. C. (2005) Akt1/protein kinase Bα is critical for ischemic and VEGF-mediated angiogenesis. *J. Clin. Invest.* **115,** 2119–2127
12. Chen, J., Somanath, P. R., Razorenova, O., Chen, W. S., Hay, N., Bornstein, P., and Byzova, T. V. (2005) Akt1 regulates pathological angiogenesis, vascular maturation and permeability *in vivo*. *Nat. Med.* **11,** 1188–1196
13. Bornstein, P. (2009) Thrombospondins function as regulators of angiogenesis. *J Cell Commun. Signal.* **3,** 189–200
14. Armstrong, L. C., and Bornstein P. (2003) Thrombospondins 1 and 2 function as inhibitors of angiogenesis. *Matrix Biol.* **22,** 63–71
15. Bornstein, P. (1992) Thrombospondins: structure and regulation of expression. *FASEB J.* **6,** 3290–3299
16. Bornstein, P. (2001) Thrombospondins as matricellular modulators of cell function. *J. Clin. Invest.* **107,** 929–934
17. Bornstein, P., Agah, A., and Kyriakides, T. R. (2004) The role of thrombospondins 1 and 2 in the regulation of cell-matrix interactions, collagen fibril formation, and the response to injury. *Int. J. Biochem. Cell Biol.* **36,** 1115–1125
18. Krady, M. M., Zeng, J., Yu, J., MacLauchlan, S., Skokos, E. A., Tian, W., Bornstein, P., Sessa, W. C., and Kyriakides, T. R. (2008) Thrombospondin-2 modulates extracellular matrix remodeling during physiological angiogenesis. *Am. J. Pathol.* **173,** 879–891
19. Kyriakides, T. R., Tam, J. W., and Bornstein, P. (1999) Accelerated wound healing in mice with a disruption of the thrombospondin 2 gene. *J. Invest. Dermatol.* **113,** 782–787
20. Agah, A., Kyriakides, T. R., Letrondo, N., Björkblom, B., and Bornstein, P. (2004) Thrombospondin 2 levels are increased in aged mice: consequences for cutaneous wound healing and angiogenesis. *Matrix Biol.* **22,** 539–547
21. Maclauchlan, S., Skokos, E. A., Agah, A., Zeng, J., Tian, W., Davidson, J. M., Bornstein, P., and Kyriakides, T. R. (2009) Enhanced angiogenesis and reduced contraction in thrombospondin-2-null wounds is associated with increased levels of matrix metalloproteinases-2 and -9, and soluble VEGF. *J. Histochem. Cytochem.* **57,** 301–313
22. Kyriakides, T. R., Zhu, Y. H., Yang, Z., Huynh, G., and Bornstein, P. (2001) Altered extracellular matrix remodeling and angiogenesis in sponge granulomas of thrombospondin 2-null mice. *Am. J. Pathol.* **159,** 1255–1262
23. Kyriakides, T. R., Leach, K. J., Hoffman, A. S., Ratner, B. D., and Bornstein, P. (1999) Mice that lack the angiogenesis inhibitor, thrombospondin 2, mount an altered foreign body reaction characterized by increased vascularity. *Proc. Natl. Acad. Sci. U.S.A.* **96,** 4449–4454
24. Simantov, R., Febbraio, M., and Silverstein, R. L. (2005) The antiangiogenic effect of thrombospondin-2 is mediated by CD36 and modulated by histidine-rich glycoprotein. *Matrix Biol.* **24,** 27–34
25. Isenberg, J. S., Annis, D. S., Pendrak, M. L., Ptaszynska, M., Frazier, W. A., Mosher, D. F., and Roberts, D. D. (2009) Differential interactions of thrombospondin-1, -2, and -4 with CD47 and effects on cGMP signaling and ischemic injury responses. *J. Biol. Chem.* **284,** 1116–1125
26. Kyriakides, T. R., Zhu, Y. H., Smith, L. T., Bain, S. D., Yang, Z., Lin, M. T., Danielson, K. G., Iozzo, R. V., LaMarca, M., McKinney, C. E., Ginns, E. I., and Bornstein, P. (1998) Mice that lack thrombospondin 2 display connective tissue abnormalities that are associated with disordered collagen fibrillogenesis, an increased vascular density, and a bleeding diathesis. *J. Cell Biol.* **140,** 419–430
27. Somanath, P. R., and Byzova, T. V., (2009) 14-3-3β-Rac1-p21 activated kinase signaling regulates Akt1-mediated cytoskeletal organization, lamellipodia formation and fibronectin matrix assembly. *J. Cell Physiol.* **218,** 394–404
28. Kimura, K., Kawamoto, K., Teranishi, S., and Nishida, T. (2006) Role of Rac1 in fibronectin-induced adhesion and motility of human corneal epithelial cells. *Invest. Ophthalmol. Vis. Sci.* **47,** 4323–4329
29. Wennerberg, K., Ellerbroek, S. M., Liu, R. Y., Karnoub, A. E., Burridge, K., and Der, C. J. (2002) RhoG signals in parallel with Rac1 and Cdc42. *J. Biol. Chem.* **277,** 47810–47817
30. Wheeler, A. P., Wells, C. M., Smith, S. D., Vega, F. M., Henderson, R. B., Tybulewicz, V. L., and Ridley, A. J. (2006) Rac1 and Rac2 regulate macrophage morphology but are not essential for migration. *J. Cell Sci.* **119,** 2749–2757
31. Cernuda-Morollón, E., and Ridley, A. J. (2006) Rho GTPases and leukocyte adhesion receptor expression and function in endothelial cells. *Circ. Res.* **98,** 757–767
32. Zhou, G. L., Tucker, D. F., Bae, S. S., Bhatheja, K., Birnbaum, M. J., and Field, J. (2006) Opposing roles for Akt1 and Akt2 in Rac/Pak signaling and cell migration. *J. Biol. Chem.* **281,** 36443–36453
33. Somanath, P. R., Kandel, E. S., Hay, N., and Byzova, T. V. (2007) Akt1 signaling regulates integrin activation, matrix recognition, and fibronectin assembly. *J. Biol. Chem.* **282,** 22964–22976
34. Byzova, T. V., Kim, W., Midura, R. J., and Plow, E. F. (2000) Activation of integrin $\alpha_V\beta_3$ regulates cell adhesion and migration to bone sialoprotein. *Exp. Cell Res.* **254,** 299–308
35. Plow, E. F., Haas, T. A., Zhang, L., Loftus, J., and Smith, J. W. (2000) Ligand binding to integrins. *J. Biol. Chem.* **275,** 21785–21788
36. Hynes, R. O. (2004) The emergence of integrins: a personal and historical perspective. *Matrix Biol.* **23,** 333–340
37. Byzova, T. V., Goldman, C. K., Pampori, N., Thomas, K. A., Bett, A., Shattil, S. J., and Plow, E. F. (2000) A mechanism for modulation of cellular responses to VEGF: activation of the integrins. *Mol. Cell* **6,** 851–860
38. Fernández-Hernando, C., József, L., Jenkins, D., Di Lorenzo, A., and Sessa, W. C. (2009) Absence of Akt1 reduces vascular smooth muscle cell migration and survival and induces features of plaque vulnerability and cardiac dysfunction during atherosclerosis. *Arterioscler. Thromb. Vasc. Biol.* **29,** 2033–2040
39. Bialkowska, K., Zaffran, Y., Meyer, S. C., and Fox, J. E. (2003) 14-3-3 ζ mediates integrin-induced activation of Cdc42 and Rac: platelet glycoprotein Ib-IX regulates integrin-induced signaling by sequestering 14-3-3 ζ. *J. Biol. Chem.* **278,** 33342–33350
40. Mammoto, A., Mammoto, T., and Ingber, D. E. (2008) Rho signaling and mechanical control of vascular development. *Curr. Opin. Hematol.* **15,** 228–234
41. ten Klooster, J. P., Jaffer, Z. M., Chernoff, J., and Hordijk, P. L. (2006) Targeting and activation of Rac1 are mediated by the exchange factor beta-Pix. *J. Cell Biol.* **172,** 759–769
42. Chittenden, T. W., Claes, F., Lanahan, A. A., Autiero, M., Palac, R. T., Tkachenko, E. V., Elfenbein, A., Ruiz de Almodovar, C., Dedkov, E., Tomanek, R., Li, W., Westmore, M., Singh, J. P., Horowitz, A., Mulligan-Kehoe, M. J., Moodie, K. L., Zhuang, Z. W., Carmeliet, P., and Simons, M. (2006) Selective regulation of arterial branching morphogenesis by synectin. *Dev. Cell* **10,** 783–795
43. Lanahan, A. A., Chittenden, T. W., Mulvihill, E., Smith, K., Schwartz, S., and Simons, M. (2006) Synectin-dependent gene expression in endothelial cells. *Physiol. Genomics* **27,** 380–390
44. Rudic, R. D., Shesely, E. G., Maeda, N., Smithies, O., Segal, S. S., and Sessa, W. C. (1998) Direct evidence for the importance of endothelium-derived nitric oxide in vascular remodeling. *J. Clin. Invest.* **101,** 731–736
45. Dimmeler, S., Fleming, I., Fisslthaler, B., Hermann, C., Busse, R., and Zeiher, A. M. (1999) Activation of nitric oxide synthase in endothelial cells by Akt-dependent phosphorylation. *Nature* **399,** 601–605
46. Schaffer, M. R., Tantry, U., Gross, S. S., Wasserburg, H. L., and Barbul, A. (1996) Nitric oxide regulates wound healing. *J. Surg. Res.* **63,** 237–240
47. Lee, P. C., Salyapongse, A. N., Bragdon, G. A., Shears, L. L., 2nd, Watkins, S. C., Edington, H. D., and Billiar, T. R. (1999) Impaired wound healing and angiogenesis in eNOS-deficient mice. *Am. J. Physiol.* **277,** H1600–H1608
48. Yu, J., deMuinck, E. D., Zhuang, Z., Drinane, M., Kauser, K., Rubanyi, G. M., Qian, H. S., Murata, T., Escalante, B., and Sessa, W. C. (2005) Endothelial nitric oxide synthase is critical for ischemic remodeling, mural cell recruitment, and blood flow reserve. *Proc. Natl. Acad. Sci. U.S.A.* **102,**

10999–11004
49. Schleicher, M., Yu, J., Murata, T., Derakhshan, B., Atochin, D., Qian, L., Kashiwagi, S., Di Lorenzo, A., Harrison, K. D., Huang, P. L., and Sessa, W. C. (2009) The Akt1-eNOS axis illustrates the specificity of kinase-substrate relationships *in vivo*. *Sci. Signal*. **2,** ra41
50. Fernández-Hernando, C., Ackah, E., Yu, J., Suárez, Y., Murata, T., Iwakiri, Y., Prendergast, J., Miao, R. Q., Birnbaum, M. J., and Sessa, W. C. (2007) Loss of Akt1 leads to severe atherosclerosis and occlusive coronary artery disease. *Cell Metab.* **6,** 446–457
51. Somanath, P. R., Razorenova, O. V., Chen, J., and Byzova, T. V. (2006) Akt1 in endothelial cell and angiogenesis. *Cell Cycle.* **5,** 512–518
52. Werner-Felmayer, G., Werner, E. R., Fuchs, D., Hausen, A., Reibnegger, G., and Wachter, H. (1990) Tetrahydrobiopterin-dependent formation of nitrite and nitrate in murine fibroblasts. *J. Exp. Med.* **172,** 1599–1607
53. Tzeng, E., Billiar, T. R., Robbins, P. D., Loftus, M., and Stuehr, D. J. (1995) Expression of human inducible nitric oxide synthase in a tetrahydrobiopterin (H4B)-deficient cell line: H4B promotes assembly of enzyme subunits into an active dimer. *Proc. Natl. Acad. Sci. U.S.A.* **92,** 11771–11775
54. Cho, H., Thorvaldsen, J. L., Chu, Q., Feng, F., and Birnbaum, M. J. (2001) Akt1/PKBα is required for normal growth but dispensable for maintenance of glucose homeostasis in mice. *J. Biol. Chem.* **276,** 38349–38352
55. Oganesian, A., Armstrong, L. C., Migliorini, M. M., Strickland, D. K., and Bornstein, P. (2008) Thrombospondins use the VLDL receptor and a nonapoptotic pathway to inhibit cell division in microvascular endothelial cells. *Mol. Biol. Cell* **19,** 563–571
56. Agah, A., Kyriakides, T. R., Lawler, J., and Bornstein, P. (2002) The lack of thrombospondin-1 (TSP1) dictates the course of wound healing in double-TSP1/TSP2-null mice. *Am. J. Pathol.* **161,** 831–839
57. Bouaouina, M., Harburger, D. S., and Calderwood, D. A. (2012) Talin and signaling through integrins. *Methods Mol. Biol.* **757,** 325–347
58. Agah, A., Kyriakides, T. R., and Bornstein, P. (2005) Proteolysis of cell-surface tissue transglutaminase by matrix metalloproteinase-2 contributes to the adhesive defect and matrix abnormalities in thrombospondin-2-null fibroblasts and mice. *Am. J. Pathol.* **167,** 81–88
59. Linnerth-Petrik, N. M., Santry, L. A., Petrik, J. J., and Wootton, S. K. (2014) Opposing functions of akt isoforms in lung tumor initiation and progression. *PLoS One* **9,** e94595
60. Gonzalez, E., and McGraw, T. E. (2009) The Akt kinases: isoform specificity in metabolism and cancer. *Cell Cycle* **8,** 2502–2508
61. Diez, H., Garrido, J. J., and Wandosell, F., (2012) Specific roles of Akt iso forms in apoptosis and axon growth regulation in neurons. *PLoS One* **7,** e32715
62. Somanath, P. R., Chen, J., and Byzova, T. V. (2008) Akt1 is necessary for the vascular maturation and angiogenesis during cutaneous wound healing. *Angiogenesis* **11,** 277–288
63. Shiojima, I., and Walsh, K. (2002) Role of Akt signaling in vascular homeostasis and angiogenesis. *Circ. Res.* **90,** 1243–1250
64. Gurtner, G. C., Werner, S., Barrandon, Y., and Longaker, M. T. (2008) Wound repair and regeneration. *Nature* **453,** 314–321
65. Liu, S., Xu, S. W., Blumbach, K., Eastwood, M., Denton, C. P., Eckes, B., Krieg, T., Abraham, D. J., and Leask, A. (2010) Expression of integrin β1 by fibroblasts is required for tissue repair *in vivo*. *J. Cell Sci.* **123,** 3674–3682
66. Singer, A. J., and Clark, R. A. (1999) Cutaneous wound healing. *N. Engl. J. Med.* **341,** 738–746
67. Lauffenburger, D. A., and Horwitz, A. F. (1996) Cell migration: a physically integrated molecular process. *Cell* **84,** 359–369
68. Ridley, A. J. (2004) Pulling back to move forward. *Cell* **116,** 357–358
69. Zaidel-Bar, R., Itzkovitz, S., Ma'ayan, A., Iyengar, R., and Geiger, B. (2007) Functional atlas of the integrin adhesome. *Nat. Cell Biol.* **9,** 858–867
70. Zaidel-Bar, R., Milo, R., Kam, Z., and Geiger, B. (2007) A paxillin tyrosine phosphorylation switch regulates the assembly and form of cell-matrix adhesions. *J. Cell Sci.* **120,** 137–148
71. Liu, S., Xu, S. W., Kennedy, L., Pala, D., Chen, Y., Eastwood, M., Carter, D. E., Black, C. M., Abraham, D. J., and Leask, A. (2007) FAK is required for TGFβ-induced JNK phosphorylation in fibroblasts: implications for acquisition of a matrix-remodeling phenotype. *Mol. Biol. Cell* **18,** 2169–2178